Trimodality imaging system and intravascular endoscopic probe: combined optical coherence tomography, fluorescence imaging and ultrasound imaging

Shanshan Liang,[1,2] Teng Ma,[3] Joseph Jing,[1,2] Xiang Li,[3] Jiawen Li,[1,2] K. Kirk Shung,[3] Qifa Zhou,[3] Jun Zhang,[1,2,4] and Zhongping Chen[1,2,5]

[1]*Beckman Laser Institute, University of California, 1002 Health Sciences Rd., Irvine, California 92617, USA*

[2]*Department of Biomedical Engineering, University of California, 5200 Engineering Hall, Irvine, California 92697, USA*

[3]*The Resource Center for Medical Ultrasonic Transducer Technology, University of Southern California, Los Angeles 90089, USA*

[4]*e-mail: junzhang@uci.edu*

[5]*e-mail: z2chen@uci.edu*

Received September 23, 2014; revised October 14, 2014; accepted October 14, 2014; posted October 24, 2014 (Doc. ID 223700); published November 21, 2014

In this Letter, we present a trimodality imaging system and an intravascular endoscopic probe for the detection of early-stage atherosclerotic plaques. The integrated system is able to acquire optical coherence tomography (OCT), fluorescence, and ultrasound images and simultaneously display them in real time. A trimodality intravascular endoscopic probe of 1.2 mm in diameter and 7 mm in length was fabricated based on a dual-modality optical probe that integrates OCT and fluorescence imaging functions and a miniature ultrasound transducer. The probe is capable of rotating at up to 600 rpm. *Ex vivo* images from rabbit aorta and human coronary arteries showed that this combined system is capable of providing high resolution, deep penetration depth and specific molecular fluorescence contrast simultaneously.

OCIS codes: (110.4190) Multiple imaging; (110.4500) Optical coherence tomography; (110.7170) Ultrasound; (170.0170) Medical optics and biotechnology; (170.2150) Endoscopic imaging; (260.2510) Fluorescence.

http://dx.doi.org/10.1364/OL.39.006652

Cardiovascular diseases contribute to the most deaths in the U.S. [1]. Atherosclerosis is the main cause of strokes, serious heart attacks, and other peripheral vascular disease. Prevention and early treatment through the detection of plaque lesions is the first and most fundamental step toward increasing the survival rate of patients with cardiovascular diseases. Many clinical studies have shown that there are three critical characteristics of vulnerable plaques. They are (a) large lipid pool, (b) thin fibrous cap, and (c) major inflammatory reaction [2,3]. In order to image and characterize vulnerable plaques, several types of intravascular probes were developed. Among all these approaches, intravascular ultrasound (IVUS) has been used most widely in clinical studies [4]. IVUS is capable of obtaining cross-section images of the blood vessel wall without blocking blood flow due to the low attenuation of ultrasound in blood. Ultrasound signal could penetrate through a whole blood vessel wall to identify atherosclerotic plaques. Therefore, it is suitable for detecting the extent of plaques. However, the resolution of the typical IVUS is usually around $50 \sim 200\,\mu m$, which is not sufficient to measure the thickness of thin fibrous cap with a typical thickness around the 50~60-μm range. On the other hand, optical coherence tomography (OCT) can provide a high-resolution, cross-section microstructure image of tissue [5]. Intravascular OCT is capable of measuring the thickness of a fibrous cap with 5~10-μm axial resolution [6]. For an intravascular study, the accurate thickness of thin fibrous caps can be assessed by using OCT images. However, OCT has a limited penetration depth of 1–2 mm, which makes it difficult to see though a vessel wall. Intravascular OCT also suffers from high optical scattering in blood; hence, flushing blood from the vessel imaging lesion with transparent media would be necessary during image acquisitions. It has been shown that OCT and IVUS provide complementary microstructure information of vulnerable plaques, including fibrous cap thickness and lipid pool size [7]. With these two imaging modalities, fine structure information of the blood vessel wall can be fully characterized. We have shown that calcified plaques can be identified with either the OCT or IVUS modality. However, there are limited molecular contrast agents for imaging other types of plaques with this structure image modality.

Fluorescence imaging is a standard method for studying molecular specifications of biological tissue composition. Therefore, intravascular fluorescence imaging endoscopy could be used for detecting specific molecular information inside atherosclerotic plaques [8]. With the presentation of different antibodies and fluorescence dyes, or even with autofluorescence, the intravascular fluorescence endoscopic probe is capable of detecting different molecular compositions that will indicate the status of atherosclerotic plaques. However, intravascular fluorescence probes usually only provide 2D-specific fluorescence signals without giving any cross-section structure information. Therefore, in order to detect more useful information in a short time and in one scan procedure, many groups have been working on multimodality intravascular imaging systems and endoscopic probes, such as OCT combined with IVUS [7], fluorescence imaging combined with OFDI [9], and FLIM combined with IVUS [10]. We have been working on an OCT combined with a fluorescence imaging system [11]. These dual modality systems are advantageous

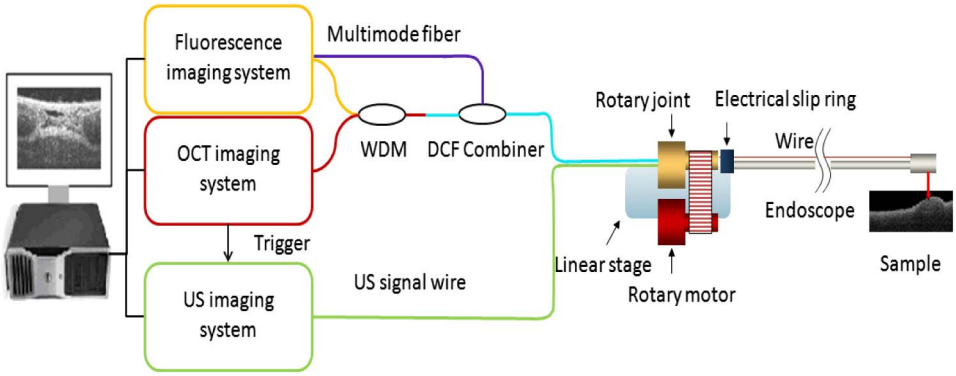

Fig. 1. Schematic of the trimodalities integrated system and for the probe. OCT and fluorescence system were combined with WDM. Ultrasound signal was synchronized with optical signal by the trigger from swept source laser.

since they can simultaneously obtain two different imaging contrast information. However, dual modality imaging systems remain unable to image and quantify all three characteristics of vulnerable plaques simultaneously.

In this study, we report the development of a trimodality intravascular imaging system that can image and quantify all three critical characteristics of vulnerable plaques and have built a trimodality intravascular imaging system. This system integrated OCT, IVUS, and fluorescence imaging modalities into a single catheter. With this trimodality system, three different types of images could be collected simultaneously, and all data could be processed in parallel though a graphics processing unit (GPU) and then displayed in real time. A trimodality endoscopic probe was fabricated based on a combined OCT and fluorescence dual-modality optical probe and a miniature side viewing ultrasound transducer. *Ex vivo* images from rabbit and human coronary arteries demonstrated the capability of this combined trimodality intravascular imaging system.

The integrated system setup is shown in Fig. 1. The trimodality imaging system is an integration of a swept-source OCT (SS-OCT) system, a fluorescence intensity imaging system, and an ultrasound imaging system. The top left part of Fig. 1 shows the optical imaging system, which includes a 1310-nm SS-OCT system and a fluorescence imaging system. The SS-OCT system has a swept source with a center wavelength of 1310 nm and a sweeping rate of 20 kHz (Santec, HSL-2100). For the fluorescence system, a 635-nm semi-conductive CW laser was used as the fluorescence excitation source. The filter set can be chosen based on the fluorescence dye used to stain the sample. In our experiments, Cy5.5 was used, which has an excitation peak around 675 nm (33% of the peak efficiency at 635 nm) and an emission peak at 690 nm. The two optical imaging systems were combined together with a wavelength division multiplexer (WDM coupler 635/1310), then the mixed light wave was coupled into a double-clad fiber (DCF) combiner (Avensys Tech). The single-mode core of the DCF was used for OCT signal transmission as well as the fluorescence excitation light delivery. When the light hits the sample and reflects back into the coupler, the OCT signal is transmitted through the single-mode core and back to the interferometer. At the same time, fluorescence emission signal is collected by the inner clad of the DCF, which has a larger diameter and higher NA; therefore, the collection efficiency of fluorescence emission light is much higher than that of the core. The fluorescence signal is coupled through the multimode port of DCF combiner and is detected by a photomultiplier tube (PMT, Hamamatsu, H9305-01). For the ultrasound part, an ultrasound pulse generator and receiver (Olympus Panametrics 5900PR) is used for ultrasound signal generation and detection. A trigger from the swept-source laser is used here to synchronize the optical part and ultrasound part. The same trigger is also used for data acquisition.

A trimodality intravascular endoscopic probe was fabricated for this multifunctional imaging system, as shown in Fig. 2. The optical part and ultrasound part were placed side by side in a metal cap piece. The optical part of this probe was a dual-modality optical probe that combined OCT and fluorescence functions together. The incident light was focused by a GRIN lens, which was placed in front of a double clad fiber, then directed to the sample by a 45-deg reflective rod mirror. The ultrasound sensor used here was a single-element ultrasound transducer with a center frequency of around 45 MHz, and the size of the element was 0.4 mm × 0.4 mm. The outer diameter of the current prototype trimodality probe is 1.2 mm. We used a proximal-end scanning mechanism. The optical rotary joint was connected to a motor, and the rotational part of the slip ring was mounted on the optical fiber connector, allowing the trimodality probe to rotate. Torque from the motor was translated to the distal end of the probe by a double-wrapped torque coil (Asahi Intec, Santa Ana, California). The rotational system was mounted on a linear stage (Zaber Technologies

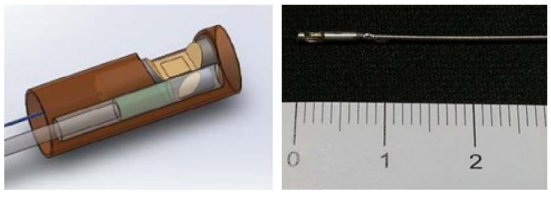

Fig. 2. Structure of the trimodality endoscopic probe: the optical probe and ultrasound transducer were placed side by side. The rigid portion of the probe is 0.7 cm and the diameter is 1.2 mm. The scale is in centimeters.

Inc., Vancouver, British Columbia), which was used for linear translation. The rotational and linear scanning mechanisms allow the system to provide 3D helical scan.

Data acquisition was carried out by two synchronized data acquisition cards (Alazar Technologies Inc., Canada) and then processed by a commercial graphical processing unit (Nvidia, Santa Clara, California) using Nvidia's CUDA package. The data processing software of our integrated system was developed to be capable of doing OCT, ultrasound, and fluorescence data acquisition, image processing, and display in real time.

In order to evaluate this trimodality intravascular imaging system, we first did *ex vivo* imaging of a normal New Zealand white rabbit aorta in which two model plaques had been planted inside the blood vessel wall. The model plaques were formed by injecting a mixture of saturated grease and cholesterol. The two model plaques were injected side by side next to each other: one of them only contained only the fatty mixture, and the other one was mixed with 0.1 μmol/L Cy5.5 dye. After testing the model plaques in the rabbit aorta, we also imaged *ex vivo* human cadaver artery. The segment of tissue was stained with Annexin V-conjugated Cy5.5 for over 24 h and then soaked in saline for another 24 h to get rid of unattached fluorescence molecules. Annexin V was used to target apoptotic macrophages that accumulated in the necrotic core [12]. Before imaging, the tissue sample was fixed by formalin and preserved in PBS.

Images of the model plaques that formed inside normal New Zealand rabbit are shown in Fig. 3. Figure 3(a) is the structure diagram of the model plaques and shows the relative location of the two model plaques. Figures 3(b)–3(d) are the intravascular OCT combined fluorescence image, IVUS combined fluorescence image, and combined trimodality image. Figures 3(e)–3(g) are the 3D OCT and fluorescence combined image, 3D ultrasound combined fluorescence image, and 3D combined trimodality image, respectively.

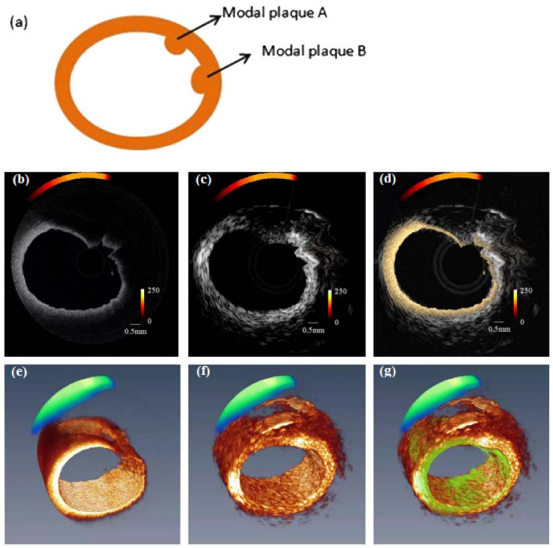

Fig. 3. *Ex vivo* images from two modal plaques injected in rabbit aorta (a) schematic of two modal plaques, (b) OCT combined fluorescence image, (c) ultrasound structure image-combined fluorescence, (d) combined OCT, ultrasound, and fluorescence image, (e) 3D reconstruction of OCT-combined fluorescence, (f) 3D ultrasound and fluorescence image, and (g) 3D-combined trimodality image.

Since the ultrasound and optical probes are placed side by side, there will be a small angular shift when the combined probe rotates. This offset can be corrected by rotating the ultrasound image. The ultrasound images could provide structure information over the full depth of the vessel wall. With an axial resolution of around 40 μm and a lateral resolution of around 420 μm, it is difficult to tell the boundary of the plaque region from the surrounding tissue. On the other hand, the boundary of the model plaque can be distinguished clearly in the OCT image due to its high resolution (axial resolution of 8 μm and lateral resolution of 50 μm). However, the penetration depth is not sufficient to image through model plaques. By using both OCT and ultrasound images, the microstructure of the model plaques can be revealed clearly. However, we were still unable to distinguish the two model plaques from the structure images. Fluorescence signal alone was unable to reveal the model plaques due to lack of structure information, and the coregistration of fluorescence signal and OCT image helps indicate the molecular difference. From the combined image, we can easily tell that model plaque A is mixed with fluorescence dye and model plaque B is without fluorescence dye. The model plaque experiment showed that the trimodality system is capable of simultaneously obtaining OCT, ultrasound, and fluorescence images and displaying them in real time.

Figure 4 illustrates the combined *ex vivo* images from a human cadaver coronary artery sample stained with Annexin V conjugated Cy5.5. The ultrasound images show the whole structure including the entire shape of the blood vessel wall. In contrast to the ultrasound images, the OCT image shows the fine structure of the vessel wall and provides a much clearer layer structure. The fluorescence signal indicates the area where the Annexin V conjugated Cy5.5 exists. These regions usually contain a higher concentration of phosphatidylserine that can be used to target apoptosis. During the formation of a necrotic core, large amounts of macrophage infiltrate the core and undergo apoptosis [12]. Different target agents can be chosen based on pathological information of high-risk vulnerable plaques.

In this Letter, a trimodality imaging system and multimodal intravascular endoscopic probe were presented. The integrated system is capable of obtaining OCT, ultrasound, and fluorescence data simultaneously and displaying images in real time. The intravascular endoscopic probe for this integrated system was fabricated based on a single-element ultrasound transducer and a

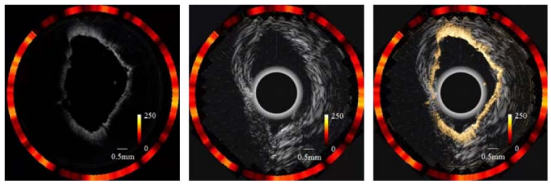

Fig. 4. *Ex vivo* images from human coronary artery (a) combined OCT and fluorescence image, (b) combined ultrasound and fluorescence image, and (c) combined trimodality image.

dual-modality OCT/fluorescence optical probe. *Ex vivo* studies show that this trimodality system is capable of obtaining a high-resolution OCT cross-section image, deep-penetration-depth ultrasound structure image, and a specific molecular fluorescence signal. These three modalities can be used as the three critical criteria for diagnoses of vulnerable plaques. The system also can be matched with other types of multi-modality endoscopic systems to help diagnose other diseases in the future, such as diseases of the digestive tract or urethra.

In order to use the trimodality system for human intravascular *in vivo* studies, the diameter of the probe must be reduced from the current size of 1.2 to 1 mm or less.. In addition, to shorten the length of imaging time during operations, we are working on increasing the imaging speed to 3000 rpm where a 5-cm-long vessel can be scanned in 4 s with an interframe spacing of 250 μm. For *in vivo* studies, we can further reduce the flushing time by adopting a strategy of using IVUS first for the preliminary diagnosis and then only flushing the suspected lesions to obtain high-resolution optical images afterward. Finally, for *in vivo* studies, a guide wire and proper imaging sheath with flushing mechanism will be implemented.

This work was supported by National Institutes of Health under grants R01EB-10090, R01HL-125084, R01HL-105215, R01EY-021519, P41-EB002182, P41EB-015890, K25HL-102055, and TRDRP 19KT-0034. The authors would like to thank the individuals who donated their bodies and tissues for the advancement of research.

References

1. S. Yusuf, S. Reddy, S. Ounpuu, and S. Anand, Circulation **104**, 2746 (2001).
2. M. Naghavi, P. Libby, E. Falk, S. W. Casscells, S. Litovsky, J. Rumberger, J. J. Badimon, C. Stefanadis, P. Moreno, G. Pasterkamp, Z. Fayad, P. H. Stone, S. Waxman, P. Raggi, M. Madjid, A. Zarrabi, A. Burke, C. Yuan, P. J. Fitzgerald, D. S. Siscovick, C. L. de Korte, M. Aikawa, A. K. Juhani, G. Assmann, C. R. Becker, J. H. Chesebro, A. Farb, S. Galis, C. Jackson, I. K. Jang, W. Koenig, R. A. Lodder, K. March, J. Demirovic, M. Navab, S. G. Priori, M. D. Rekhter, R. Bahr, S. M. Grundy, R. Mehran, A. Colombo, E. Boerwinkle, C. Ballantyne, W. J. Insull, R. S. Schwartz, R. Vogel, P. W. Serruys, G. K. Hansson, D. P. Faxon, S. Kaul, H. Drexler, P. Greenland, J. E. Muller, R. Virmani, P. M. Ridker, D. P. Zipes, P. K. Shah, and J. T. Willerson, Circulation **108**, 1664 (2003).
3. P. Libby and T. Pierre, Circulation **111**, 3481 (2005).
4. G. S. Mintz, H. M. Garcia-Garcia, S. J. Nicholls, N. J. Weissman, N. Bruining, T. Crowe, J. C. Tardif, and P. W. Serruys, EuroIntervention **6**, 1123 (2011).
5. J. G. Fujimoto, M. E. Brezinski, G. J. Tearney, S. A. Boppart, B. Bouma, M. R. Hee, J. F. Southern, and E. A. Swanson, Nat. Med. **1**, 970 (1995).
6. I. K. Jang, B. E. Bouma, D. H. Kang, S. J. Park, S. W. Park, K. B. Seung, K. B. Choi, M. Shishkov, K. Schlendorf, E. Pomerantsev, S. L. Houser, H. T. Aretz, and G. J. Tearney, J. Am. Coll. Cardiol. **39**, 604 (2002).
7. J. Yin, X. Li, J. Jing, J. Li, D. Mukai, S. Mahon, A. Edris, K. Hoang, K. K. Shung, M. Brenner, J. Narula, Q. Zhou, and Z. Chen, J. Biomed. Opt. **16**, 60505 (2011).
8. F. A. Jaffer, M. A. Calfon, A. Rosenthal, G. Mallas, R. N. Razansky, A. Mauskapf, R. Weissleder, P. Libby, and V. Ntziachristos, J. Am. Coll. Cardiol. **57**, 2516 (2011).
9. H. Yoo, J. W. Kim, M. Shishkov, E. Namati, T. Morse, R. Shubochkin, J. R. McCarthy, V. Ntziachristos, B. E. Bouma, F. A. Jaffer, and G. J. Tearney, Nat. Med. **17**, 1680 (2011).
10. J. Bec, H. Xie, D. R. Yankelevich, F. Zhou, Y. Sun, N. Ghata, R. Aldredge, and L. Marcu, J. Biomed. Opt. **7**, 106012 (2012).
11. S. Liang, A. Saidi, J. Jing, G. Liu, J. Li, J. Zhang, C. Sun, J. Narula, and Z. Chen, J. Biomed. Opt. **7**, 70501 (2012).
12. P. Libby, P. M. Ridker, and A. Maseri, Circulation **105**, 1135 (2002).